

A search for extremely-high-energy neutrinos with IceCube and implications for the ultra-high-energy cosmic-ray proton fraction

The IceCube Collaboration

(a complete list of authors can be found at the end of the proceedings)

E-mail: mmeier@icecube.wisc.edu, brianclark@icecube.wisc.edu

When ultra-high-energy cosmic rays (UHECRs) interact with ambient photon backgrounds, a flux of extremely-high-energy (EHE), so-called cosmogenic, neutrinos is produced. The observation of these neutrinos with IceCube can probe the nature of UHECRs. We present a search for EHE neutrinos using 12.6 years of IceCube data. The non-observation of neutrinos with energies $\gtrsim 10$ PeV constrains the all-flavor neutrino flux at 1 EeV to be below $E^2 \Phi_{\nu_e + \nu_\mu + \nu_\tau} \simeq 10^{-8}$ GeV cm $^{-2}$ s $^{-1}$ sr $^{-1}$, the most stringent limit to date. This constrains the proton fraction in UHECRs of energy above 30 EeV to be $\lesssim 70\%$ if the evolution of the UHECR sources is similar to the star formation rate. Our analysis circumvents uncertainties associated with hadronic interaction models in studies of UHECR air showers, which also suggest a heavy composition at such energies.

Corresponding authors: Maximilian Meier^{1*}, Brian A. Clark²¹ Chiba University² University of Maryland, College Park

* Presenter

*The 39th International Cosmic Ray Conference (ICRC2025)
14 – 24 July, 2025
Geneva, Switzerland*

1. Introduction

Extremely-high-energy (EHE, $E_\nu \gtrsim 10$ PeV) neutrinos are unique messengers of the high redshift universe. Other Standard Model messenger particles do not arrive at Earth from high redshifts due to attenuation by their interactions with background photon fields. Neutrinos on the other hand carry no charge and only interact weakly, allowing them to reach Earth undeflected and unattenuated. EHE neutrinos are expected to be produced in interactions of ultra-high-energy cosmic rays (UHECRs): Either during their propagation through the universe, interacting with cosmic microwave background photons, called *cosmogenic neutrinos*, or by cosmic-ray interactions in environments close to their astrophysical sources themselves, called *astrophysical neutrinos*. The cosmogenic neutrino flux encodes unique information about the sources of UHECRs — its shape and normalization can provide information about the chemical composition of UHECRs, the redshift evolution of their sources, and the maximum acceleration energy of the cosmic ray accelerators. In this work, we report on a search for EHE neutrinos based on 12.6 years of IceCube data [1].

The IceCube Neutrino Observatory [2] is a cubic kilometer of deep ice at the geographic South Pole instrumented with 5160 Digital Optical Modules (DOMs), distributed on 86 strings, each housing a photomultiplier tube and readout electronics. Additionally, a surface array called IceTop [3], deployed on top of the IceCube strings, measures cosmic-ray air showers. Neutrino interactions produce charged particles that give rise to Cherenkov light when they propagate through the ice. The Cherenkov light is recorded by the detector and can be used to reconstruct the arrival direction and energy of the neutrinos. EHE neutrinos are observed in IceCube as tracks — μ/τ leptons originating from charged-current (CC) interactions of ν_μ/ν_τ depositing light while propagating through the ice — or cascades — roughly spherical energy depositions from ν_e CC or neutral-current interactions.

2. Event Selection

The IceCube data is dominated by atmospheric muon bundles that trigger the detector at a rate of about 3 kHz, while the expected rate of cosmogenic neutrinos is constrained to be much smaller than 1 event per year. An event selection is applied to select high-energy neutrinos, focusing on neutrino energies greater than 10 PeV, while rejecting atmospheric neutrino and muon backgrounds (for a detailed description, see [1]). Cosmogenic neutrino events have extremely high energy, depositing a large amount of light or equivalently charge. The atmospheric muon background is exclusively down-going, and thus a majority of the background can be removed with a charge threshold depending on the reconstructed arrival direction of the event. Another key difference between high-energy neutrino signals and atmospheric muon bundles is their energy loss profile. The energy loss profiles of single high-energy muons show large stochastic variations, while in high-multiplicity muon bundles these fluctuations partly average out. This information is included by reconstructing energy loss profiles along the reconstructed track directions and imposing more strict charge thresholds for less stochastic events. Finally, events are vetoed if they show activity in the IceTop surface array in temporal coincidence with the reconstructed track.

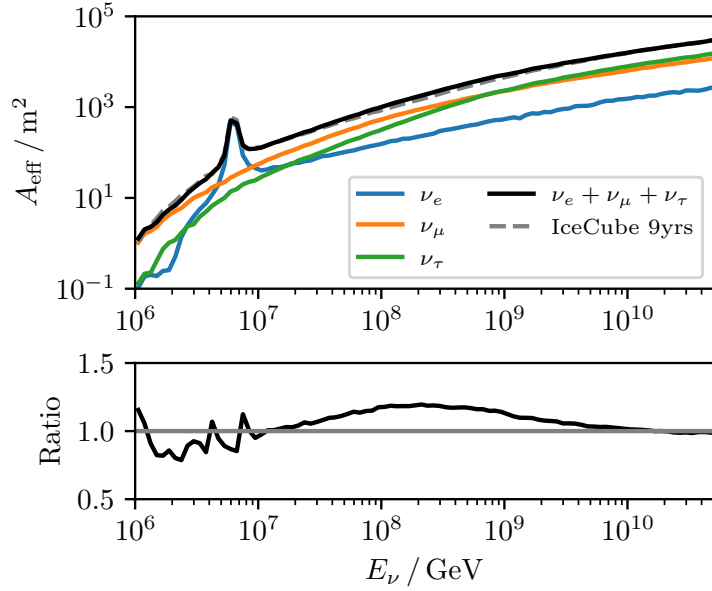


Figure 1: The 4π - $\nu/\bar{\nu}$ averaged effective area of the event selection. The effective area of a previous search, IceCube 9yrs from [4], is shown as a dashed line for comparison.

The effective area of the event selection is shown in Fig. 1 averaging the whole sky and the contributions from neutrinos and anti-neutrinos. This new event selection improves the effective area between 100 PeV and 1 EeV by about 15 % due to the inclusion of stochasticity information. In addition to improvements in effective area, the analyzed livetime is increased by about 50 % to a total of 4605 days.

After applying this event selection, the background expected in the analyzed livetime consists of 0.40 ± 0.03 events from atmospheric sources and between ~ 9 [5] and ~ 0.5 ($\gamma = 2.39$, $E_{\text{cutoff}} = 1.4$ PeV [6]) astrophysical neutrinos depending on the assumed spectral behavior of astrophysical neutrinos. For the construction of upper limits described here, the parameters $\gamma = 2.39$ and $E_{\text{cutoff}} = 1.4$ PeV are assumed for astrophysical flux, described a power law with an exponential cutoff, because this leads to conservative results. Three data events, consistent with the expectation from astrophysical background, survive the event selection.

3. Analysis and Results

The sample is analyzed by splitting events into subsets made up of tracks and cascades and binning them based on their reconstructed energy and arrival direction. Then, a binned Poisson likelihood is used to fit the data:

$$\mathcal{L}(\lambda_{\text{GZK}}, \lambda_{\text{astro}}) = \prod_i \text{Pois}(n_i | \lambda_{\text{GZK}} \mu_{\text{GZK},i} + \lambda_{\text{astro}} \mu_{\text{astro},i} + \mu_{\text{bkg},i}), \quad (1)$$

where λ_{GZK} is a relative normalization to a signal flux of cosmogenic neutrinos and λ_{astro} is a nuisance parameter scaling the astrophysical neutrino flux. n_i describes the observed number of events in bin i , and μ_i describes the expectation for a signal model, the astrophysical background

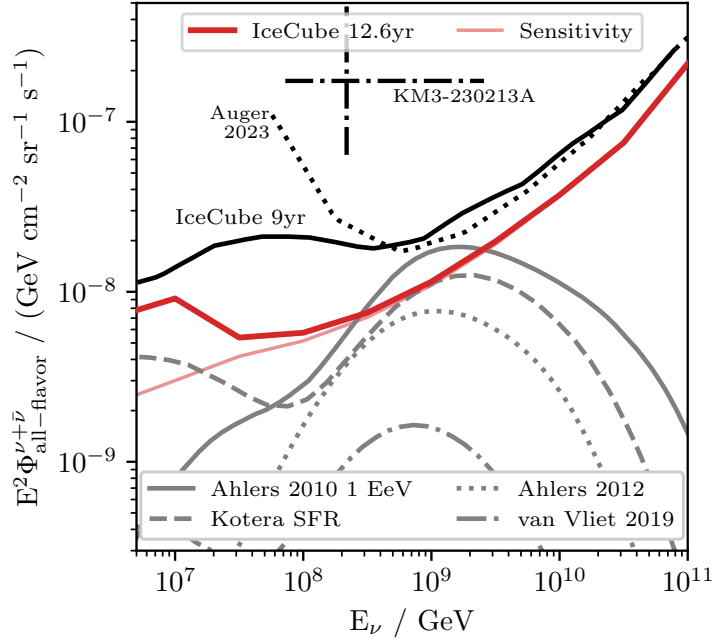


Figure 2: Differential limit at 90% CL on the all-flavor neutrino flux. The limit is compared to the IceCube result based on 9 years of data [4], the limit by Auger [8] and to a few cosmogenic flux models [9–12]. The model labeled van Vliet 2019 assumes $\alpha = 2.5$, $E_{\max} = 10^{20}$ eV, $m = 3.4$ and a proton fraction of 10%. The limit from Auger has been re-scaled to decade-wide bins for an easier comparison.

and the sum of all atmospheric background respectively. A generic differential limit on the EHE neutrino flux beyond the astrophysical expectation is obtained by injecting a sliding E^{-1} flux with a width of one decade. Additionally, specific signal models can also be tested using a likelihood-ratio test statistic. All hypothesis tests are based on ensembles of pseudoexperiments and confidence intervals are constructed based on the method described in [7].

The differential limit obtained in this work is shown in Fig. 2 as a red line as well as the sensitivity, i.e. the limit obtained in case of a null observation. Below about 100 PeV the limit is weakened with respect to the sensitivity due to the observed events.

Since the known flux of astrophysical neutrinos has been taken into account in the construction of the differential limit, the limit applies to any component of the UHE neutrino flux, whether it is cosmogenic neutrinos or a, so far unknown, component of UHE neutrinos produced directly in astrophysical sources.

3.1 Implications for the UHECR proton fraction

Based on the observed flux of UHECRs, the non-observation of cosmogenic neutrinos imposes interesting constraints on the sources of UHECRs, in particular the UHECR proton fraction [13]. The connection between UHECRs and cosmogenic neutrinos is modeled using CRPropa simulation [14] and follows the method laid out in [12] with a detailed description given in [1]. The predicted cosmogenic neutrino flux depends mainly on the composition of UHECRs, the flux of UHECRs injected by their sources, and the source distribution as a function of redshift. The

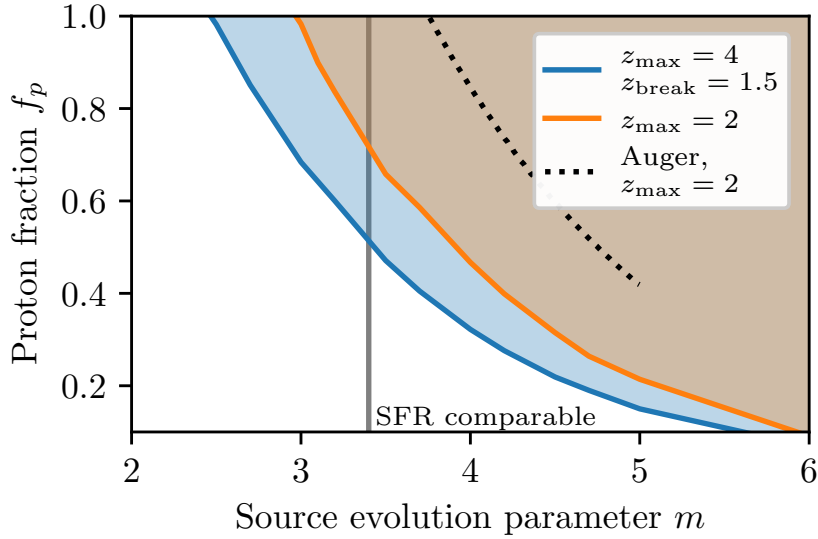


Figure 3: Constraints on the UHECR proton fraction as a function of the source evolution parameter m at 90% CL. The excluded region is shown for the two described source evolution models $SE_1(z)$ (blue), and $SE_2(z)$ (orange), and compared to constraints based on the non-observation of neutrinos in Auger [15].

injected flux is modeled conservatively, where spectral parameters are chosen to minimize the expected neutrino flux. For the cosmological source evolution two different models are tested:

$$SE_1(z) = \begin{cases} (1+z)^m, & z \leq z' \\ (1+z')^m, & z > z' \end{cases} \quad (2)$$

with $z' = 1.5$ and $z_{\max} = 4$, and a more conservative model $SE_2(z) = (1+z)^m$ with $z_{\max} = 2$, where z denotes the redshift and m the so-called source evolution parameter.

The resulting constraints on the proton fraction above ~ 30 EeV are shown in Fig. 3 as a function of the source evolution parameter. Since neutrinos can probe the distant universe, the proton fraction and the value of m are degenerate. For instance, if the UHECR source evolution is comparable to the star formation rate (SFR) or stronger, the proton fraction is constrained to be below about 70%.

Direct air shower measurements already strongly constrain the composition of UHECRs to be heavy [16, 17], and even favor the total absence of protons in the highest energy bin [18]. Still, some analyses find that an additional proton component that contributes up to $\sim 10\%$ to the total UHECR flux can improve the fit to the data compared to a one population model [19, 20]. The contribution can be reduced to the percent level by considering different hadronic interaction models. Regardless, in these scenarios the redshift evolution is not constrained when considering cosmic-ray observations alone. Neutrinos can effectively probe sources with large redshifts and a significant fraction of cosmogenic neutrinos originate from UHECR protons produced in sources with $z > 1$. This effectively allows for a measurement of the proton fraction as a function of m . For source classes with strong redshift evolution, such as high-luminosity AGN [21] ($m = 7.1$) the

constraints derived in this work are competitive with the proton fractions allowed by cosmic-ray data.

4. KM3-230213A

Recently, the KM3NeT Collaboration published an EHE neutrino candidate with an estimated energy of ~ 220 PeV [22]. This single event leads to an inferred diffuse neutrino flux in an energy range from 72 PeV to 2.6 EeV of $E^2\Phi_{\text{all-flavor}} = 1.74 \times 10^{-7} \text{ GeV cm}^{-2} \text{ s}^{-1} \text{ sr}^{-1}$ assuming that the flux follows E^{-2} . The flux is also shown in Fig. 2 and significantly exceeds the limits set in this work. This flux corresponds to an expectation of ~ 70 events, which is inconsistent with a non-observation in the quoted energy range at the level of more than 10σ .

This tension can be significantly reduced by considering the global picture of high-energy neutrino detectors. A joint fit combining the observation of KM3NeT with the non-observation of neutrinos in the same energy range by IceCube and Auger [23] reduces the tension based on the hypothesis of a diffuse flux to 2.6σ [22, 24]. The joint fit in [22] uses the IceCube exposure from [4]. We repeat the joint fit including the IceCube exposure presented in this work. The probability of the joint fit flux of $E^2\Phi_{\text{all-flavor}} = 1.7 \times 10^{-9} \text{ GeV cm}^{-2} \text{ s}^{-1} \text{ sr}^{-1}$ resulting in an observation with one event in KM3NeT, and no events in both Auger and IceCube is $\sim 0.35\%$. The goodness-of-fit p-value is determined to be 0.4% (2.9σ) based on the saturated Poisson likelihood ratio test [25].

This tension motivates to check whether IceCube is observing similarly spectacular near-horizontal events that could have been removed by the event selection summarized in Sec. 2. Fig. 4 shows a rather low-level distribution of the charge for events reconstructed to be close to horizontal with $|\cos(\theta)| \leq 0.1$. No other selection has been applied except for the lower charge requirement of $Q \geq 10^4$ PE. The simulation sum for different cosmic-ray primary composition models (GaisserH3a, proton only or iron only composition) is compared to the data represented by black points. No excess of events is observed above the combination of atmospheric backgrounds and astrophysical neutrinos. Additionally, the brown line shows the predicted charge distribution for a cosmogenic flux model. The distribution has a long tail to small charges, but an event similar to KM3-230213A where a muon with an energy of $\mathcal{O}(100 \text{ PeV})$ passes through the detector with a favorable geometry can easily produce charges on the order of 10^6 PE.

5. Conclusion

The non-observation of EHE neutrinos in 12.6 years of IceCube data places the strongest constraints to date on the flux of the highest energy neutrinos, reaching a flux at 1 EeV of $E^2\Phi \simeq 10^{-8} \text{ GeV cm}^{-2} \text{ s}^{-1} \text{ sr}^{-1}$. Additionally, this observation can constrain the UHECR composition, disfavoring a proton-only composition if the UHECR source evolution is comparable to or stronger than the star formation rate.

Planned projects utilizing the radio detection technique for neutrinos [26, 27] will reach neutrino fluxes about 1.5 orders of magnitude smaller than the current IceCube limit at 1 EeV, probing cosmogenic neutrinos to significantly smaller proton fractions. The combination of a measurement of the cosmogenic neutrino flux with a proton fraction measurement from future cosmic ray detectors can be used to constrain the source evolution of potential pure-proton sources of UHECRs [20].

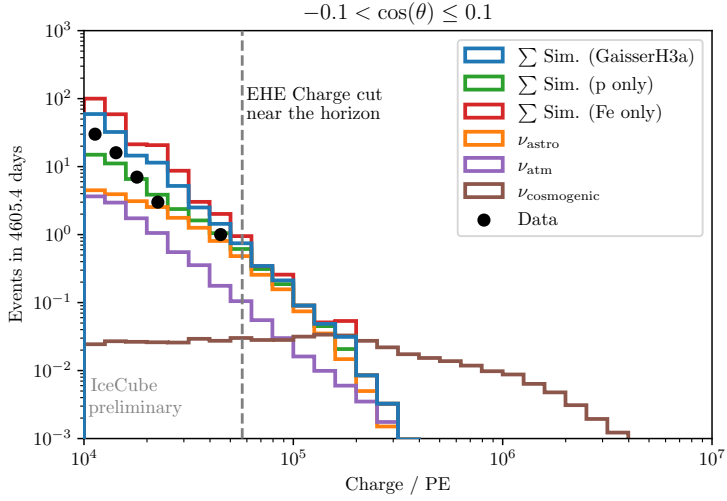


Figure 4: Charge distribution for events reconstructed close to the horizon with $-0.1 < \cos(\theta) \leq 0.1$. Except for the lower charge requirement of the histogram at $Q \geq 10^4$ PE no selection criteria have been applied. The lines labeled \sum Sim combine the predictions for atmospheric muons, neutrinos and astrophysical neutrinos (assuming a single power law with cutoff: $\gamma = 2.52$, $E_{\text{cutoff}} = 1.4$ PeV [6]). The distribution for cosmogenic neutrinos is plotted separately using the same model as the dash-dotted line in Fig. 2 [12].

References

- [1] **IceCube** Collaboration, R. Abbasi *et al.*, *PRL* (2025, to be published).
- [2] **IceCube** Collaboration, M. Aartsen *et al.*, *JINST* **12** (2017) P03012.
- [3] **IceCube** Collaboration, R. Abbasi *et al.*, *Nucl. Instrum. Methods Phys. Res. A* **700** (2013) 188–220.
- [4] **IceCube** Collaboration, M. Aartsen *et al.*, *Phys. Rev. D* **98** (2018) 062003.
- [5] **IceCube** Collaboration, R. Abbasi *et al.*, *ApJ* **928** (2022) 50.
- [6] R. Naab, E. Ganster, Z. Zhang, *et al.*, *PoS ICRC2023* (2023) 1064.
- [7] G. J. Feldman and R. D. Cousins, *Phys. Rev. D* **57** (1998) 3873.
- [8] M. Niechciol *et al.*, *PoS ICRC2023* (2023) 1488.
- [9] M. Ahlers, L. Anchordoqui, M. Gonzalez-Garcia, F. Halzen, and S. Sarkar, *Astropart. Phys.* **34** (2010) 106–115.
- [10] K. Kotera, D. Allard, and A. V. Olinto, *JCAP* **10** (2010) 013.
- [11] M. Ahlers and F. Halzen, *Phys. Rev. D* **86** (2012) 083010.
- [12] A. van Vliet, R. A. Batista, and J. R. Hörandel, *Phys. Rev. D* **100** (2019) 021302.
- [13] M. Ahlers, L. A. Anchordoqui, and S. Sarkar, *Phys. Rev. D* **79** (2009) 083009.

- [14] R. Alves Batista *et al.*, *JCAP* **09** (2022) 035.
- [15] **Pierre Auger** Collaboration, A. Aab *et al.*, *JCAP* **10** (2019) 022.
- [16] **Pierre Auger** Collaboration, A. Abdul Halim *et al.*, *JCAP* **05** (2023) 024.
- [17] **Telescope Array** Collaboration, R. Abbasi *et al.*, *Phys. Rev. Lett.* **133** (2024) 041001.
- [18] J. Bellido *et al.*, *PoS ICRC2017* (2017) 506.
- [19] D. Ehlert, A. van Vliet, F. Oikonomou, and W. Winter, *JCAP* **02** (2024) 022.
- [20] M. S. Muzio, M. Unger, and S. Wissel, *Phys. Rev. D* **107** (2023) 103030.
- [21] G. Hasinger, T. Miyaji, and M. Schmidt, *Astronomy & Astrophysics* **441** (2005) 417–434.
- [22] **KM3NeT** Collaboration, S. Aiello *et al.*, *Nature* **638** (2025) 376–382.
- [23] **Pierre Auger** Collaboration, A. Aab *et al.*, *Journal of Cosmology and Astroparticle Physics* **11** (2019) 004.
- [24] **KM3NeT** Collaboration, O. Adriani *et al.*, *Phys. Rev. X* (2025, to be published) .
- [25] S. Baker and R. D. Cousins, *Nucl. Instrum. Methods Phys. Res.* **221** (1984) 437–442.
- [26] **IceCube-Gen2** Collaboration, R. Abbasi *et al.*, “IceCube Gen2: Technical Design Report,” 2023. <https://icecube-gen2.wisc.edu/science/publications/tdr/>.
- [27] K. Fang *et al.*, *PoS ICRC2017* (2018) 996.

Full Author List: IceCube Collaboration

R. Abbasi¹⁶, M. Ackermann⁶³, J. Adams¹⁷, S. K. Agarwalla^{39, a}, J. A. Aguilar¹⁰, M. Ahlers²¹, J.M. Alameddine²², S. Ali³⁵, N. M. Amin⁴³, K. Andeen⁴¹, C. Argüelles¹³, Y. Ashida⁵², S. Athanasiadou⁶³, S. N. Axani⁴³, R. Babu²³, X. Bai⁴⁹, J. Baines-Holmes³⁹, A. Balagopal V.^{39, 43}, S. W. Barwick²⁹, S. Bash²⁶, V. Basu⁵², R. Bay⁶, J. J. Beatty^{19, 20}, J. Becker Tjus^{9, b}, P. Behrens¹, J. Beise⁶¹, C. Bellenghi²⁶, B. Benkel⁶³, S. BenZvi⁵¹, D. Berley¹⁸, E. Bernardini^{47, c}, D. Z. Besson³⁵, E. Blaufuss¹⁸, L. Bloom⁵⁸, S. Blot⁶³, I. Bodo³⁹, F. Bontempo³⁰, J. Y. Book Motzkin¹³, C. Boscolo Meneguolo^{47, c}, S. Böser⁴⁰, O. Botner⁶¹, J. Böttcher¹, J. Braun³⁹, B. Brinson⁴, Z. Brisson-Tsavoussi³², R. T. Burley², D. Butterfield³⁹, M. A. Campana⁴⁸, K. Carloni¹³, J. Carpio^{33, 34}, S. Chattopadhyay^{39, a}, N. Chau¹⁰, Z. Chen⁵⁵, D. Chirkin³⁹, S. Choi⁵², B. A. Clark¹⁸, A. Coleman⁶¹, P. Coleman¹, G. H. Collin¹⁴, D. A. Coloma Borja⁴⁷, A. Connolly^{19, 20}, J. M. Conrad¹⁴, R. Corley⁵², D. F. Cowen^{59, 60}, C. De Clercq¹¹, J. J. DeLaunay⁵⁹, D. Delgado¹³, T. Delmeulle¹⁰, S. Deng¹, P. Desiati³⁹, K. D. de Vries¹¹, G. de Wasseige³⁶, T. DeYoung²³, J. C. Díaz-Vélez³⁹, S. DiKerby²³, M. Dittmer⁴², A. Domí²⁵, L. Draper⁵², L. Dueser¹, D. Durnford²⁴, K. Dutta⁴⁰, M. A. DuVernois³⁹, T. Ehrhardt⁴⁰, L. Eidenschink²⁶, A. Eimer²⁵, P. Eller²⁶, E. Ellinger⁶², D. Elsässer²², R. Engel^{30, 31}, H. Erpenbeck³⁹, W. Esmail⁴², S. Eulig¹³, J. Evans¹⁸, P. A. Evenson⁴³, K. L. Fan¹⁸, K. Fang³⁹, K. Farrag¹⁵, A. R. Fazely⁵, A. Fedynitch⁵⁷, N. Feigl⁸, C. Finley⁵⁴, L. Fischer⁶³, D. Fox⁵⁹, A. Franckowiak⁹, S. Fukami⁶³, P. Fürst¹, J. Gallagher³⁸, E. Ganster¹, A. Garcia¹³, M. Garcia⁴³, G. Garg^{39, a}, E. Genton^{13, 36}, L. Gerhardt⁷, A. Ghadimi⁵⁸, C. Glaser⁶¹, T. Glüsenkamp⁶¹, J. G. Gonzalez⁴³, S. Goswami^{33, 34}, A. Granados²³, D. Grant¹², S. J. Gray¹⁸, S. Griffin³⁹, S. Griswold⁵¹, K. M. Groth²¹, D. Guevel³⁹, C. Günther¹, P. Gutjahr²², C. Ha⁵³, C. Haack²⁵, A. Hallgren⁶¹, L. Halve¹, F. Halzen³⁹, L. Hamacher¹, M. Ha Minh²⁶, M. Handt¹, K. Hanson³⁹, J. Hardin¹⁴, A. A. Harnisch²³, P. Hatch³², A. Haungs³⁰, J. Häußler¹, K. Helbing⁶², J. Hellrung⁹, B. Henke²³, L. Hennig²⁵, F. Henningsen¹², L. Heuermann¹, R. Hewett¹⁷, N. Heyer⁶¹, S. Hickford⁶², A. Hidvegi⁵⁴, C. Hill¹⁵, G. C. Hill², R. Hmaid¹⁵, K. D. Hoffman¹⁸, D. Hooper³⁹, S. Hori³⁹, K. Hoshina^{39, d}, M. Hostert¹³, W. Hou³⁰, T. Huber³⁰, K. Hultqvist⁵⁴, K. Hymon^{22, 57}, A. Ishihara¹⁵, W. Iwakiri¹⁵, M. Jacquart²¹, S. Jain³⁹, O. Janik²⁵, M. Jansson³⁶, M. Jeong⁵², M. Jin¹³, N. Kamp¹³, D. Kang³⁰, W. Kang⁴⁸, X. Kang⁴⁸, A. Kappes⁴², L. Kardum²², T. Karg⁶³, M. Karl²⁶, A. Karle³⁹, A. Katil²⁴, M. Kauer³⁹, J. L. Kelley³⁹, M. Khanal⁵², A. Khatee Zathul³⁹, A. Kheirandish^{33, 34}, H. Kimku⁵³, J. Kiryluk⁵⁵, C. Klein²⁵, S. R. Klein^{6, 7}, Y. Kobayashi¹⁵, A. Kochcocki²³, R. Koiral⁴³, H. Kolanoski⁸, T. Kontrimas²⁶, L. Köpke⁴⁰, C. Kopper²⁵, D. J. Koskinen²¹, P. Koundal⁴³, M. Kowalski^{8, 63}, T. Kozynets²¹, N. Krieger⁹, J. Krishnamoorthi^{39, a}, T. Krishnan¹³, K. Kruiswijk³⁶, E. Krupczak²³, A. Kumar⁶³, E. Kun⁹, N. Kurahashi⁴⁸, N. Lad⁶³, C. Lagunas Gualda²⁶, L. Lallement Arnaud¹⁰, M. Lamoureux³⁰, M. J. Larson¹⁸, F. Lauber⁶², J. P. Lazar³⁶, K. Leonard DeHolton⁶⁰, A. Leszczyńska⁴³, J. Liao⁴, C. Lin⁴³, Y. T. Liu⁶⁰, M. Liubarska²⁴, C. Love⁴⁸, L. Lu³⁹, F. Lucarelli²⁷, W. Luszczak^{19, 20}, Y. Lyu^{6, 7}, J. Madsen³⁹, E. Magnus¹¹, K. B. M. Mahn²³, Y. Makino³⁹, E. Manao²⁶, S. Mancina^{47, e}, A. Mand³⁹, I. C. Maris¹⁰, S. Marka⁴⁵, Z. Marka⁴⁵, L. Marten¹, I. Martinez-Soler¹³, R. Maruyama⁴⁴, J. Mauro³⁶, F. Mayhew²³, F. McNally³⁷, J. V. Mead²¹, K. Meagher³⁹, S. Mechbal⁶³, A. Medina²⁰, M. Meier¹⁵, Y. Merckx¹¹, L. Merten⁹, J. Mitchell⁵, L. Molchany⁴⁹, T. Montaruli²⁷, R. W. Moore²⁴, Y. Morii¹⁵, A. Mosbrugger²⁵, M. Mouhai³⁹, D. Mousadi⁶³, E. Moyaux³⁶, T. Mukherjee³⁰, R. Naab⁶³, M. Nakos³⁹, U. Naumann⁶², J. Necker⁶³, L. Neste⁵⁴, M. Neumann⁴², H. Niederhausen²³, M. U. Nisa²³, K. Noda¹⁵, A. Noell¹, A. Novikov⁴³, A. Obertacke Pollmann¹⁵, V. O'Dell³⁹, A. Olivas¹⁸, R. Orsoe²⁶, J. Osborn³⁹, E. O'Sullivan⁶¹, V. Palusova⁴⁰, H. Pandya⁴³, A. Parenti¹⁰, N. Park³², V. Parrish²³, E. N. Paudel⁵⁸, L. Paul⁴⁹, C. Pérez de los Heros⁶¹, T. Pernice⁶³, J. Peterson³⁹, M. Plum⁴⁹, A. Pontén⁶¹, V. Poojyam⁵⁸, Y. Popovich⁴⁰, M. Prado Rodriguez³⁹, B. Pries²³, R. Procter-Murphy¹⁸, G. T. Przybyski⁷, L. Pyras⁵², C. Raab³⁶, J. Rack-Helleis⁴⁰, N. Rad⁶³, M. Ravn⁶¹, K. Rawlins³, Z. Rechav³⁹, A. Rehman⁴³, I. Reistroffer⁴⁹, E. Resconi²⁶, S. Reusch⁶³, C. D. Rho⁵⁶, W. Rhode²², L. Ricca³⁶, B. Riedel³⁹, A. Rifai⁶², E. J. Roberts², S. Robertson^{6, 7}, M. Rongen²⁵, A. Rosted¹⁵, C. Rott⁵², T. Ruhe²², L. Ruohan²⁶, D. Ryckbosch²⁸, J. Saffer³¹, D. Salazar-Gallegos²³, P. Sampathkumar³⁰, A. Sandrock⁶², G. Sanger-Johnson²³, M. Santander⁵⁸, S. Sarkar⁴⁶, J. Savelberg¹, M. Scarnera³⁶, P. Schaile²⁶, M. Schaufel¹, H. Schieles³⁰, S. Schindler²⁵, L. Schlückmann⁴⁰, B. Schlüter⁴², F. Schlüter¹⁰, N. Schmeisser⁶², T. Schmidt¹⁸, F. G. Schröder^{30, 43}, L. Schumacher²⁵, S. Schwirn¹, S. Scalfani¹⁸, D. Seckel⁴³, L. Seen³⁹, M. Seikh³⁵, S. Seunarine⁵⁰, P. A. Sevle Myhr³⁶, R. Shah⁴⁸, S. Shefali³¹, N. Shimizu¹⁵, B. Skrzypek⁶, R. Snihur³⁹, J. Soedingrekso²², A. Søgaard²¹, D. Soldin⁵², P. Soldin¹, G. Sommani⁹, C. Spannfellner²⁶, G. M. Spiczak⁵⁰, C. Spiering⁶³, J. Stachurska²⁸, M. Stamatikos²⁰, T. Staney⁴³, T. Stezelberger⁷, T. Stürwald⁶², T. Stuttard²¹, G. W. Sullivan¹⁸, I. Taboada⁴, S. Ter-Antonyan⁵, A. Terliuk²⁶, A. Thakuri⁴⁹, M. Thiesmeyer³⁹, W. G. Thompson¹³, J. Thwaites³⁹, S. Tilay⁴³, K. Tollefson²³, S. Toscano¹⁰, D. Tosi³⁹, A. Trettin⁶³, A. K. Upadhyay^{39, a}, K. Upshaw⁵, A. Vaidyanathan⁴¹, N. Valtonen-Mattila^{9, 61}, J. Valverde⁴¹, J. Vandembroucke³⁹, T. van Eeden⁶³, N. van Eijndhoven¹¹, L. van Rootselaar²², J. van Santen⁶³, F. J. Vara Carbonell⁴², F. Varsi³¹, M. Venugopal³⁰, M. Vereecken³⁶, S. Vergara Carrasco¹⁷, S. Verpoest⁴³, D. Veske⁴⁵, A. Vijai¹⁸, J. Villarreal¹⁴, C. Walck⁵⁴, A. Wang⁴, E. Warrick⁵⁸, C. Weaver²³, P. Weigel¹⁴, A. Weindl³⁰, J. Weldert⁴⁰, A. Y. Wen¹³, C. Wendt³⁹, J. Werthebach²², M. Weyrauch³⁰, N. Whitehorn²³, C. H. Wiebusch¹, D. R. Williams⁵⁸, L. Witthaus²², M. Wolf²⁶, G. Wrede²⁵, X. W. Xu⁵, J. P. Yanéz²⁴, Y. Yao³⁹, E. Yildizci³⁹, S. Yoshida¹⁵, R. Young³⁵, F. Yu¹³, S. Yu⁵², T. Yuan³⁹, A. Zegarelli⁹, S. Zhang²³, Z. Zhang⁵⁵, P. Zilberman³⁹

¹ III. Physikalisches Institut, RWTH Aachen University, D-52056 Aachen, Germany

² Department of Physics, University of Adelaide, Adelaide, 5005, Australia

³ Dept. of Physics and Astronomy, University of Alaska Anchorage, 3211 Providence Dr., Anchorage, AK 99508, USA

⁴ School of Physics and Center for Relativistic Astrophysics, Georgia Institute of Technology, Atlanta, GA 30332, USA

⁵ Dept. of Physics, Southern University, Baton Rouge, LA 70813, USA

⁶ Dept. of Physics, University of California, Berkeley, CA 94720, USA

⁷ Lawrence Berkeley National Laboratory, Berkeley, CA 94720, USA

⁸ Institut für Physik, Humboldt-Universität zu Berlin, D-12489 Berlin, Germany

⁹ Fakultät für Physik & Astronomie, Ruhr-Universität Bochum, D-44780 Bochum, Germany

¹⁰ Université Libre de Bruxelles, Science Faculty CP230, B-1050 Brussels, Belgium

- ¹¹ Vrije Universiteit Brussel (VUB), Dienst ELEM, B-1050 Brussels, Belgium
¹² Dept. of Physics, Simon Fraser University, Burnaby, BC V5A 1S6, Canada
¹³ Department of Physics and Laboratory for Particle Physics and Cosmology, Harvard University, Cambridge, MA 02138, USA
¹⁴ Dept. of Physics, Massachusetts Institute of Technology, Cambridge, MA 02139, USA
¹⁵ Dept. of Physics and The International Center for Hadron Astrophysics, Chiba University, Chiba 263-8522, Japan
¹⁶ Department of Physics, Loyola University Chicago, Chicago, IL 60660, USA
¹⁷ Dept. of Physics and Astronomy, University of Canterbury, Private Bag 4800, Christchurch, New Zealand
¹⁸ Dept. of Physics, University of Maryland, College Park, MD 20742, USA
¹⁹ Dept. of Astronomy, Ohio State University, Columbus, OH 43210, USA
²⁰ Dept. of Physics and Center for Cosmology and Astro-Particle Physics, Ohio State University, Columbus, OH 43210, USA
²¹ Niels Bohr Institute, University of Copenhagen, DK-2100 Copenhagen, Denmark
²² Dept. of Physics, TU Dortmund University, D-44221 Dortmund, Germany
²³ Dept. of Physics and Astronomy, Michigan State University, East Lansing, MI 48824, USA
²⁴ Dept. of Physics, University of Alberta, Edmonton, Alberta, T6G 2E1, Canada
²⁵ Erlangen Centre for Astroparticle Physics, Friedrich-Alexander-Universität Erlangen-Nürnberg, D-91058 Erlangen, Germany
²⁶ Physik-department, Technische Universität München, D-85748 Garching, Germany
²⁷ Département de physique nucléaire et corpusculaire, Université de Genève, CH-1211 Genève, Switzerland
²⁸ Dept. of Physics and Astronomy, University of Gent, B-9000 Gent, Belgium
²⁹ Dept. of Physics and Astronomy, University of California, Irvine, CA 92697, USA
³⁰ Karlsruhe Institute of Technology, Institute for Astroparticle Physics, D-76021 Karlsruhe, Germany
³¹ Karlsruhe Institute of Technology, Institute of Experimental Particle Physics, D-76021 Karlsruhe, Germany
³² Dept. of Physics, Engineering Physics, and Astronomy, Queen's University, Kingston, ON K7L 3N6, Canada
³³ Department of Physics & Astronomy, University of Nevada, Las Vegas, NV 89154, USA
³⁴ Nevada Center for Astrophysics, University of Nevada, Las Vegas, NV 89154, USA
³⁵ Dept. of Physics and Astronomy, University of Kansas, Lawrence, KS 66045, USA
³⁶ Centre for Cosmology, Particle Physics and Phenomenology - CP3, Université catholique de Louvain, Louvain-la-Neuve, Belgium
³⁷ Department of Physics, Mercer University, Macon, GA 31207-0001, USA
³⁸ Dept. of Astronomy, University of Wisconsin—Madison, Madison, WI 53706, USA
³⁹ Dept. of Physics and Wisconsin IceCube Particle Astrophysics Center, University of Wisconsin—Madison, Madison, WI 53706, USA
⁴⁰ Institute of Physics, University of Mainz, Staudinger Weg 7, D-55099 Mainz, Germany
⁴¹ Department of Physics, Marquette University, Milwaukee, WI 53201, USA
⁴² Institut für Kernphysik, Universität Münster, D-48149 Münster, Germany
⁴³ Bartol Research Institute and Dept. of Physics and Astronomy, University of Delaware, Newark, DE 19716, USA
⁴⁴ Dept. of Physics, Yale University, New Haven, CT 06520, USA
⁴⁵ Columbia Astrophysics and Nevis Laboratories, Columbia University, New York, NY 10027, USA
⁴⁶ Dept. of Physics, University of Oxford, Parks Road, Oxford OX1 3PU, United Kingdom
⁴⁷ Dipartimento di Fisica e Astronomia Galileo Galilei, Università Degli Studi di Padova, I-35122 Padova PD, Italy
⁴⁸ Dept. of Physics, Drexel University, 3141 Chestnut Street, Philadelphia, PA 19104, USA
⁴⁹ Physics Department, South Dakota School of Mines and Technology, Rapid City, SD 57701, USA
⁵⁰ Dept. of Physics, University of Wisconsin, River Falls, WI 54022, USA
⁵¹ Dept. of Physics and Astronomy, University of Rochester, Rochester, NY 14627, USA
⁵² Department of Physics and Astronomy, University of Utah, Salt Lake City, UT 84112, USA
⁵³ Dept. of Physics, Chung-Ang University, Seoul 06974, Republic of Korea
⁵⁴ Oskar Klein Centre and Dept. of Physics, Stockholm University, SE-10691 Stockholm, Sweden
⁵⁵ Dept. of Physics and Astronomy, Stony Brook University, Stony Brook, NY 11794-3800, USA
⁵⁶ Dept. of Physics, Sungkyunkwan University, Suwon 16419, Republic of Korea
⁵⁷ Institute of Physics, Academia Sinica, Taipei, 11529, Taiwan
⁵⁸ Dept. of Physics and Astronomy, University of Alabama, Tuscaloosa, AL 35487, USA
⁵⁹ Dept. of Astronomy and Astrophysics, Pennsylvania State University, University Park, PA 16802, USA
⁶⁰ Dept. of Physics, Pennsylvania State University, University Park, PA 16802, USA
⁶¹ Dept. of Physics and Astronomy, Uppsala University, Box 516, SE-75120 Uppsala, Sweden
⁶² Dept. of Physics, University of Wuppertal, D-42119 Wuppertal, Germany
⁶³ Deutsches Elektronen-Synchrotron DESY, Platanenallee 6, D-15738 Zeuthen, Germany
^a also at Institute of Physics, Sachivalaya Marg, Sainik School Post, Bhubaneswar 751005, India
^b also at Department of Space, Earth and Environment, Chalmers University of Technology, 412 96 Gothenburg, Sweden
^c also at INFN Padova, I-35131 Padova, Italy
^d also at Earthquake Research Institute, University of Tokyo, Bunkyo, Tokyo 113-0032, Japan
^e now at INFN Padova, I-35131 Padova, Italy

Acknowledgments

The authors gratefully acknowledge the support from the following agencies and institutions: USA – U.S. National Science Foundation-Office of Polar Programs, U.S. National Science Foundation-Physics Division, U.S. National Science Foundation-EPSCoR, U.S. National Science Foundation-Office of Advanced Cyberinfrastructure, Wisconsin Alumni Research Foundation, Center for High Throughput Computing (CHTC) at the University of Wisconsin-Madison, Open Science Grid (OSG), Partnership to Advance Throughput Computing (PATh), Advanced Cyberinfrastructure Coordination Ecosystem: Services & Support (ACCESS), Frontera and Ranch computing project at the Texas Advanced Computing Center, U.S. Department of Energy-National Energy Research Scientific Computing Center, Particle astrophysics research computing center at the University of Maryland, Institute for Cyber-Enabled Research at Michigan State University, Astroparticle physics computational facility at Marquette University, NVIDIA Corporation, and Google Cloud Platform; Belgium – Funds for Scientific Research (FRS-FNRS and FWO), FWO Odysseus and Big Science programmes, and Belgian Federal Science Policy Office (Belspo); Germany – Bundesministerium für Forschung, Technologie und Raumfahrt (BMFTR), Deutsche Forschungsgemeinschaft (DFG), Helmholtz Alliance for Astroparticle Physics (HAP), Initiative and Networking Fund of the Helmholtz Association, Deutsches Elektronen Synchrotron (DESY), and High Performance Computing cluster of the RWTH Aachen; Sweden – Swedish Research Council, Swedish Polar Research Secretariat, Swedish National Infrastructure for Computing (SNIC), and Knut and Alice Wallenberg Foundation; European Union – EGI Advanced Computing for research; Australia – Australian Research Council; Canada – Natural Sciences and Engineering Research Council of Canada, Calcul Québec, Compute Ontario, Canada Foundation for Innovation, WestGrid, and Digital Research Alliance of Canada; Denmark – Villum Fonden, Carlsberg Foundation, and European Commission; New Zealand – Marsden Fund; Japan – Japan Society for Promotion of Science (JSPS) and Institute for Global Prominent Research (IGPR) of Chiba University; Korea – National Research Foundation of Korea (NRF); Switzerland – Swiss National Science Foundation (SNSF).